Paper No. 973023
An ASAE Meeting Presentation

EFFECT OF WHEAT KERNEL SIZE AND ORIENTATION ON REFLECTANCE SPECTRA AND SINGLE KERNEL COLOR CLASSIFICATION

by

D. Wang
USDA Research Fellow
Texas A&M University
College Station, Texas

F. E. Dowell
Agricultural Engineer
USDA-ARS GMPRC
Manhattan, Kansas

R. E. Lacey
Assistant Professor
Texas A&M University
College Station, Texas

Written for Presentation at the
1997 ASAE Annual International Meeting
Sponsored by ASAE

Minneapolis Convention Center
Minneapolis, Minnesota
August 10-14, 1997

Summary:

An optical radiation measurement system, which measured reflectance spectra from 400 to 2000 nm, was used to determine the effect of wheat kernel size and orientation on visible and near-infrared reflectance spectral measurement. The results show that wheat kernel size and orientation had a significant effect on the spectra. Mathematical methods can be used to reduce the effect of kernel size and orientation on the spectra. The effect of kernel size and orientation on single wheat kernel color classification was tested.

Keywords:

Wheat, near-infrared, reflectance, color

ABSTRACT

An optical radiation measurement system was used to measure reflectance spectra of single wheat kernels from 400 nm to 2000 nm. Six classes of wheat were used for this study. Three kernel sizes (large, medium, and small) and three orientations (crease side, 90 degrees, and dorsal side) were used to determine how wheat kernel size and orientation affect the visible and near-infrared (NIR) reflectance spectra and single wheat kernel color classification. The results show that wheat kernel size and orientation significantly affect visible and NIR reflectance spectral measurement when the distance between a reflectance surface and the end of optical fiber was kept constant. The amount of radiation reflected by wheat kernels increased as kernel size increased. The predicted values of red and white kernels decreased as kernel size decreased. The kernel color varies with kernel orientation. The dorsal side had more effect on the wheat color classification than the crease side and side view. Some data pretreatments such as Multiplicative Scatter Correction (MSC), first and second derivative, first derivative with MSC, and second derivative with MSC could be used to reduce the effect of kernel size and orientation on the reflectance spectral data. The wavelengths with significant effects on spectral data were also found. Six-term multiple linear regression models show a strong correlation between kernel weight and absorbance in the NIR region with r^2 from 0.76 to 0.92.

INTRODUCTION

Many factors affect the accuracy of NIR reflectance spectroscopy for the analysis of agricultural products such as grains. Although the NIR technique is a simple process (no weighing is necessary, and there are no reagents to prepare), nearly 40 sources of error have been identified (Williams and Norris, 1990). Of these, sample factors and operational factors are the two major error sources affecting measurement accuracy. Williams (1975) and Williams and Thompson (1978) indicated that the most important factors affecting the accuracy of NIR reflectance spectroscopy for the analysis of ground wheat samples were the mean particle size and particle size distribution. Other important factors include sample temperature (Williams et al., 1982), moisture and protein content related to the sample used in a calibration (Williams and Thompson, 1978; Watson et al., 1977), and the growing environment of wheat (Watson et al., 1977). The growing environment causes large variations in kernel size, kernel size distribution, kernel density, and even kernel color in each wheat class. These variations affect spectral measurement by influencing the absorption of radiation by the wheat sample.

Kernel size can influence the spectral measurement by affecting the F-number (Equation 1).

$$F = \frac{f}{D} \tag{1}$$

Where f is the focal length, and D is the diameter of a lens. The radiant flux ϕ_c increases as the inverse of the square of the F-number (shown in Equation 2).

$$\phi_c = \frac{1}{F^2} \tag{2}$$

The smaller the F-number the more radiant flux (ϕ_c) will be collected by the lens. In order to get high accuracy during the measurement, the focal length f must be kept constant. However, the variation in kernel size and orientation will cause the focal length to change during measurement.

Also, different kernel sizes and orientations will result in different illumination and reflectance areas and directions. Therefore, wheat kernel size and orientation not only affect the distance between a reflectance surface and the end of optical fiber that is used to collect reflectance radiation, but also affects illumination and reflectance area and direction. Norris and Williams (1984) studied the effect of particle size of ground hard red spring wheat samples on spectral measurement. They found that sample-induced errors in NIR reflectance spectral analysis could be caused by the variation of the sample surface. They reported that the log 1/R values were significantly affected by particle size. The coarser samples have higher absorption. The particle size effect was greater at longer wavelengths. They found that the second derivative divided by second derivative at optimum wavelengths gave the best performance in predicting protein content of hard red spring wheat samples that varied widely in particle size.

Current research using NIR has shifted from ground and bulk sample analysis to single-kernel analysis and from NIR transmittance to NIR reflectance. Reflectance measurements are easier to implement in a rapid, single-kernel quality instrument (Delwiche and Massie, 1996). In order to meet those changes and obtain high accuracy, the effect of grain physical properties such as kernel size, kernel weight, and kernel orientation on spectral measurement must be clear. The purpose of this study is to identify the effect of wheat kernel size and orientation on single wheat kernel reflectance spectra and single wheat kernel color classification, and to find methods to reduce the effect of kernel size and orientation on the reflectance spectra.

MATERIALS AND METHODS

Six classes of wheat, hard red spring wheat (HRS), hard red winter wheat (HRW), soft red winter wheat (SRW), hard white wheat (HWW), soft white wheat (SWW), and durum (DUR) supplied by the Federal Grain Inspection Service (FGIS) Technical Center (Kansas City, MO), were used. The wheat samples used for measuring the effect of kernel size and orientation on the reflectance spectra are shown in Tables 1 and 2. The wheat samples used to develop calibration equations for single wheat color classification were shown in Table 3.

Single wheat kernel reflectance spectra were collected with an optical radiation measurement system (Oriel Corporation, Stratford, CT) from 400 to 2000 nm at 2 nm intervals (Figure 1). The reflectance spectra from 550 to 1900 nm were used for data analysis. The radiation source was a QTH lamp (12 V DC, 100 W). Chopped radiation was delivered by a 2-mm optical liquid fiber with F#=1 to illuminate a single wheat kernel. The illumination fiber was oriented 45 degrees from vertical with the fiber end 8 mm from the kernel. The reflectance fiber was oriented vertically above the wheat kernel with the fiber end 6 mm from the wheat kernel (Figure 2). The grating was blazed at the wavelength of 750 nm with a groove density of 600 lines per millimeter and a reciprocal dispersion of 13.2 nm/mm. The primary grating wavelengths are 450 to 2000 nm with a usable range of 400 to 2000. Identical entrance and exit slits for the monochromator were set at a height of 12 mm and width of 1.56 mm, respectively, resulting in a bandpass of 10 nm. A lead sulfide detector was used to measure the single wheat kernel reflectance from 400 to 2000 nm. Reflectance readings were referenced to a standard baseline created using spectralon which has 99% reflectivity (Labsphere, North Sutton, NH). In order to avoid the baseline changes with time, the baseline was collected once per hour. The detector constant time and pause time were set at 0.3 and 1 second, respectively.

A single wheat kernel was suspended horizontally from the germ end by a vacuum tube. For measuring the effect of kernel size on the spectral measurement, the crease side of the kernel was viewed. For measuring the effect of kernel orientation on the spectral measurement, three orientations, crease side (0 degrees), 90 degrees, and dorsal side (180 degrees), were viewed. The single kernel spectra used to develop calibration models for single wheat color classification were collected from the crease side. In order to keep the distance constant between a reflectance surface of a wheat kernel and the end of optical fiber, a three dimensional Multi-Axis Precision Translator (Newport Corporation, Irvine, CA) was used to adjust kernel position. In order to get proper orientation, a Waveplate/Polarizer Holder (Newport Corporation, Irvine, CA) was used to adjust kernel orientation from 0 to 360 degrees.

The spectral data were first transferred to log(1/R) form using the software package "Gram/32" (Galactic Industries Co., Salem, NH) and stored in Grams/32 format. The spectral data were smoothed using the Savitsky-Golay smoothing method (Savitsky and Golay, 1964). This method uses a convolution approach which performs a least square fit to a specified window of data points. Smoothing is controlled by the degree of polynomial and number of smoothing points parameters. A 5-degree polynomial with 25 points was used for smoothing the spectral region from 400-2000 nm and a 5-degree polynomial with 45 points was used for smoothing a spectral region from 1450-2000 nm, respectively. The first derivative and second derivative were also based on Savitsky-Golay method. Derivatives are an approach to addressing two of the basic problems with near-infrared spectra: overlapping peaks and large baseline variations (Williams and Norris, 1990). A 5-degree polynomial with 25 points was used to calculate the first and second derivatives. Mean centering was used to remove some variation from the data and tended to scale the data such that the mathematics of the spectral decomposition and correlations perform better. This involves calculating the average of all the spectra in the training set and then subtracting the result from each spectrum. Multiplicated scatter correction (MSC) was used to reduce the effect of kernel size and orientation on the reflectance spectra. MSC is designed to correct indeterminate path length effects caused by scattering. MSC is calculated by regressing each training spectrum against an ideal spectrum (the average of all the spectra) and by removing the slope and offset effects.

The transformation of reflectance spectra to L*a*b color system was based on Commission International de l'Eclairage (CIE) weighted-ordinate integration method and color difference formula (Hunter and Harold, 1987). The standard observer functions (CIE, 1931) were used to convert the spectral curves into tristimulus values, X, Y, and Z, that properly identify the color of an object in the terms of a mixture of the primary color that match it visually. X, Y, and Z values were then used to calculate *L*, *a*, and *b* values.

All data were analyzed using partial least squares (PLS) regression and multiple linear regression (MLR). PLS is a multivariate data analysis technique designed to handle intercorrelated regressors. It can be used to solve complicated, multivariate systems analysis problems by a sequence of simple least-squares regressions. PLS uses the concentration information during the decomposition processing. This causes spectra containing higher constituent concentrations to be weighted more heavily than those with low concentrations and gets as much concentration information as possible into the first few loading vectors. In actuality, PLS takes advantage of the correlation relationship that already exists between the spectral data and the constituent concentrations. A more complete discussion of PLS is included in Williams and Norris (1990) and Burns and Ciurczak (1991). The software package Grams/32 was used for PLS analysis. A three-class PLS model was developed to identify the effects of kernel size on the reflectance spectra. In each class, the large kernel was assigned a constant value of 1.0, medium kernel was assigned a constant value of 2.0, and small kernel was assigned a constant value of 3.0, respectively. During the model testing, a kernel was considered to be correctly categorized if the predicted value lay on the same side of the midpoint as its assigned value. MLR analysis consisted of a stepwise search of all wavelengths within a 450-1900 nm region to find the wavelengths affected significantly by kernel weight. Near-infrared model performance is reported as the multiple coefficient of determination (r^2) and standard error of calibration (SEC) of each calibration. The number of factors reported is based on the t-test and is the minimum required to give the maximum multiple coefficient of determination.

RESULTS AND DISCUSSION

1. Effect of kernel size and kernel weight on the reflectance spectra

In single kernel reflectance measurement, the illumination area is one of the most important factors affecting the errors caused by kernel size variation. The averaged spectral curves show that amount of radiation reflected by wheat kernels increased as kernel size increased (Figure 3). This result may be caused by small kernels losing some radiation energy to the background.

The effect of kernel size on the reflectance spectral measurement was determined by the multiple linear relationship between kernel size and absorbance (Log 1/R) using the three-class PLS classification models. In the near-infrared region, the results indicated that the kernel size had strong linear relationship with r^2 of 0.677 to 0.779 when the Log (1/R) values were used (Table 4). In the visible region, the results also indicate that the effects of kernel size on the reflectance spectra were significant with r^2 of 0.506 to 0.690 (Table 5). The percentage of kernels correctly classified by size shows that the highest percentage of correct classification was in the NIR region (Table 6). This indicates that the kernel size had more effect on the NIR region than in the visible region.

The effects of kernel size on the reflectance spectra can be reduced by some data pre-treatments (Table 4 and 5). Table 4 shows that all of the data pre-treatments significantly ($p < 0.05$) reduced the effect of kernel size on the NIR reflectance spectra regardless of the individual pre-treatment or the combination of the pre-treatments. However, the second derivative and second derivative with MSC were the most powerful method for reducing the effect of kernel size on the NIR reflectance spectra. Table 5 shows that all of the treatments could be used to reduce the effects of kernel size on the reflectance spectra in the visible region regardless of pre-treatment method. In general, Log (1/R) with MSC and second derivative of MSC are the most effective methods in reducing the effect of kernel size on the reflectance spectra in the visible region.

In addition to the mathematical treatments, the sample collection and preparation are also very important. Very large and very small kernels should be avoided for two major reasons. First, larger kernels will reflect more radiation, and smaller kernels will reflect less radiation. This may increase the variation in Log (1/R) values. Second, the percentage of the very large and very small kernels in the whole wheat population is small and would not significantly affect the true results.

Kernel size was related to the kernel weight. Large kernels have more mass than small kernels. The amount of radiation reflected by wheat kernels increased as the kernel weight decreased (Figure 4). Results based on the PLS calibration models indicate that kernel weight had a strong linear relationship with absorbance (log 1/R) (Table 7). Kernel weight had stronger effect in the NIR region than in the visible region. The range of r^2 in the NIR region was from 0.75 to 0.85, and the range of r^2 in the visible region was from 0.30 to 0.64. Kernel weight had more effect on hard red winter wheat with the large r^2 of 0.854 and a small SEC of 2.95. The wavelengths affected significantly by kernel weight were found by stepwise regression method. All of the wavelengths listed in table 8 were affected significantly by kernel weight ($p < 0.05$) except durum ($p < 0.10$). More than 80% of the wavelengths affected by kernel weight were in the NIR region. This also indicated that the kernel weight had a stronger effect in the NIR region. Kernel weight effect was also analyzed by six-term multiple linear regression (MLR) models (Table 9). The kernel weight can be predicted by MLR with r^2 of 0.76 to 0.92 and SEC of 6.95 to 2.37.

2. Effect of kernel orientation on the spectral measurement

The absorption curve indicates that the kernel orientation not only caused the absorption curve to shift up and down, but also caused absorption curve overlap (Figure 5). This result may be caused by two reasons. First, the kernel shape varies with kernel orientation. The crease side is relatively flat while the 90 degree side and dorsal side have angles. This will cause the changes of the direction of reflectance angles. Second, the constituents of a wheat kernel are not very uniform in the different part of the wheat kernel. The germ is located in dorsal size and the germ size of soft wheat kernels is larger than the hard wheat kernels. Also, from kernel structure, the pigment strain is located in the crease side. This may cause the crease side to be darker than the dorsal size. The color variation in the different orientations of the wheat kernel was measured by *a* values. In L*a*b color space, the *a* value represents red color for positive values. The results prove that the crease side was redder than the dorsal side (Table 10). Some *a* values of the 90 degrees view were larger than that of crease side. This probably was due to the illumination area of the 90 degrees side being smaller than the area of crease side and dorsal side.

The effect of kernel orientation on the spectral measurement could be reduced by some data pre-treatments and mathematical methods. These include MSC on Log (1/R), first derivative, and first derivative on MSC. Figure 6 shows MSC method could be used to reduce the effect of kernel orientation on the reflectance spectra. The performance of first derivative and first derivative on MSC on reducing the effect of kernel orientation will be discussed in effect of kernel orientation on the single wheat kernel color classification.

3. Effect of kernel size and orientation on the single wheat kernel color classification

The effect of kernel size and orientation on the single wheat kernel color classification was tested by the calibration equation developed by partial least squares (PLS) methods (Table 11). The percentage of large red and small white kernels misclassified increased when the Log (1/R) values were used (Table 12). For red wheat, the large size kernels had larger predicted values and more misclassified kernels than medium size and small size kernels. For white wheat, the small kernels had smaller predicted values and more misclassified kernels than large and medium kernels. The dorsal side had more effect on the wheat color classification (Table 13). The predicted values of dorsal side are larger than crease side and 90 degrees side. As discussed earlier, the pigment strain is located in the crease side. The redness of dorsal side is lighter than crease side. That is why the kernel orientation had more effect on the red wheat and some red kernels were misclassified into white wheat.

Some data pre-treatment could be used to reduce the effect of kernel size and orientation on the single wheat kernel color classification (Table 14 and 15). MSC on Log (1/R), first derivative, and first derivative on MSC could be used to reduce the effect of kernel size on the single wheat kernel color classification (Table 14). In the visible region, when the Log (1/R) values were used for single wheat kernel color classification, the percentage of misclassified kernels was 4%; after using first derivative, the percentage of misclassified kernels was 2.4%. In the visible and NIR region, when the log (1/R) values were used for single wheat kernel color classification, the percentage of misclassified kernels was 4%; after using MSC method, the percentage of misclassified kernels was 2.1%. MSC on Log (1/R) and first derivative on MSC were more powerful to reduce the effect of kernel orientation on the single wheat kernel color classification (Table 15). In the visible region, when the Log (1/R) values were used, the percentage of total misclassified kernels was 12.5%; after using MSC on Log (1/R) and first derivative on MSC, the percentage of misclassified kernels was reduced to 3.7% and 4.3, respectively. The selection of wavelength regions was also very important in reducing the effect of kernel orientation on the single wheat kernel color classification. The best results were obtained from 500 to 1700 nm. For example, with Log (1/R) in the visible region, the percentage of total misclassified kernels was 12.5%; when both visible and near-infrared regions were used, the percentage of misclassified kernels was reduced to 6.7%. This result would be explained as that spectrum in both visible and near-infrared regions may represent both outer and inner properties of a wheat kernel. However, these differences are negated when using the first derivative on the MSC.

CONCLUSIONS

Wheat kernel size and orientation had a significant effect on visible and NIR reflectance spectral data because the illumination area and reflectance direction change with kernel size and orientation. The amount of radiation reflected by the wheat kernel increased as kernel size increased. The amount of radiation absorbed by the wheat kernel varied with kernel orientation. This may introduce error into reflectance spectral data and reduce the accuracy of analysis. Some data pre-treatments such as MSC, first and second derivative, first derivative with MSC, and second derivative with MSC could be used to reduce the effect of kernel size and orientation on the reflectance spectral data. In the visible region, the effect of kernel size can be reduced easily by some mathematical methods. In the NIR regions, the most powerful methods are the second derivative and second derivative with MSC. The kernel weight has similar effects on the reflectance spectral data. The amount of radiation reflected by wheat kernel increased as kernel weight increased. The kernel size had stronger effect on spectral data in the NIR region than in the visible region. This may indicate that kernel size may have significant effect on wheat constituent analysis. Six-term multiple linear regression models show the strong correlation between kernel weight and absorbance (Log 1/R) in the NIR region with r^2 from 0.76 to 0.92.

Kernel size and orientation had a significant effect on the single wheat kernel color classification. Predicted values increased as kernel size increased. Because of the color variation at different orientations, the dorsal side had more effect on the single kernel color classification. These effects could be reduced significantly by some mathematical methods. When MSC was applied on Log (1/R), to reduce kernel size effect, the color classification accuracy was increased from 96% to 98%. When MSC and first derivative on MSC were used to reduce kernel orientation effect in the visible region, the percentage of misclassified kernels was reduced from 12.3% to 2.1%. The wavelength selection was very important to reduce the effect of kernel orientation. The results from 500 nm to 1700 nm were much better than the results from visible region. The percentage of misclassified kernels was reduced from 12.3% to 4.7%.

REFERENCES

Burns, D. A and E. W. Ciurczak. 1991. *Handbook of Near-Infrared Analysis*. 159-180. Marcel Dekker, Inc. New York, NY.

CIE. 1931. CIE standard sources for which the CIE in 1931 specified the spectral energy distributions. Commission International de l'Eclairage, Paris.

Delwiche, S. R and D. R. Massie. 1996. Classification of wheat by visible and near-infrared reflectance from single kernels. *Cereal Chem.* 73(3):399-405.

Hunter, R. S. and Harold, R. W. 1987. *The Measurements of Appearance*. Pages 100-147. Hunter Association Laboratory, Inc. Reston, VA.

Norris, K. H and P. C. Williams. 1984. Optimization of mathematical treatment of raw near-infrared signal in the measurement of protein in hard red spring wheat. I. Influence of particle size. *Cereal Chem.* 61(2):158-165.

Savitsky, A and M. J. E. Golay. 1964. Smoothing and differentiation of data by simplified least square procedures. *Anal. Chem.* 36(8):1627-1639.

Watson, C. A., Shuey, W. C., Bariasik, O. J., and J. W. Dick. 1977. Effect of wheat class on near-infrared reflectance. *Cereal Chem.* 54(6):1264-1269.

Williams, P. C. 1975. Application of near-infrared reflectance spectroscopy to analysis of cereal grains and oilseeds. *Cereal Chem.* 52(2):561-576.

Williams, P. C. and B. N. Thompson. 1978. Influence of whole meal granularity on analysis of HRS wheat for protein and moisture by near-infrared reflectance spectroscopy (NRS). *Cereal Chem.* 55(6):1014-1037.

Williams, P. C., K. H. Norris, and W. S. Zarowski. 1982. Influence of temperature on estimation of protein and moisture in wheat by near-infrared reflectance. *Cereal Chem.* 59(6):473-477.

Williams, P. C and K. H. Norris. 1990. *Near-Infrared Technology in the Agricultural and Food Industries*. 47-49, 59-69, 143-167. American Association of Cereal Chemists, Inc. St. Paul, Minnesota.

Table 1. Samples used for determination of the effect of wheat kernel size on reflectance spectra.

Sample		No. of Kernels	Avg. width Mean	Avg. width SD	Avg. length Mean	Avg. length SD	Avg. weight(mg) Mean	Avg. weight(mg) SD
HRS[1]	1[2]	25	3.62	0.13	6.83	0.32	56.61	5.37
	2[3]	25	2.94	0.07	6.47	0.25	31.81	4.59
	3[4]	25	2.36	0.08	5.78	0.31	18.82	2.90
HRW	1	25	3.20	0.07	6.83	0.17	35.62	2.87
	2	25	2.79	0.03	6.43	0.24	26.78	2.37
	3	25	2.43	0.18	5.64	0.25	17.56	2.42
SRW	1	25	3.71	0.06	7.45	0.21	45.81	2.98
	2	25	3.25	0.03	6.89	0.12	34.66	3.03
	3	25	2.78	0.04	5.94	0.11	22.09	2.00
HWW	1	25	3.87	0.07	7.45	0.21	15.7	3.83
	2	25	3.38	0.05	7.00	0.20	44.99	3.68
	3	25	2.89	0.06	6.48	0.19	31.41	4.09
SWW	1	25	3.93	0.08	7.45	0.27	55.94	4.62
	2	25	3.35	0.08	6.81	0.29	39.07	2.10
	3	25	2.93	0.10	6.17	0.21	28.03	2.81
DUR	1	25	3.89	0.05	8.31	0.11	69.01	4.72
	2	25	3.40	0.03	7.45	0.20	47.02	4.04
	3	25	2.90	0.05	6.66	0.20	31.54	3.46

[1] HRS = hard res spring, HRW = hard red winter, SRW = soft red winter, HWW = hard white wheat, SWW = soft white wheat, DUR = durum.

[2] Large kernel size.

[3] Medium kernel size.

[4] Small kernel size.

Table 2. Samples used for the determination of the effect of kernel orientation on reflectance spectra.

Class[1]	Variety	n	MC (wt)	Protein (%)	Hardness
HRS	Yecora	25	11.08	14.16	91.1
HRW	Newton	25	11.72	11.67	65.0
SRW	FGIS_55150	25	12.77	9.93	25.3
HWW	FGIS_59290	25	9.09	11.6	69.3
SWW	FGIS_58884	25	9.32	8.70	43.8
DURUM	Monroe	25	12.46	14.95	87.0

[1] HRS = hard red spring, HRW = hard red winter, SRW = soft red winter, HWW = hard white wheat, SWW = soft white wheat, DUR = durum.

Table 3. Samples used to create partial least squares (PLS) calibration equation for single wheat kernel color classification.

Wheat class[1]	Varieties	n	Hardness	MC (%)	Protein (%)
HRS	3	75	86.7-91.1	11.80-12.50	14.10-17.30
HRW	3	75	63.6-81.2	9.42 -14.44	9.38-16.16
SRW	3	75	15.6-25.3	11.80-13.79	8.86-11.50
HWW	3	75	59.9-72.5	9.07 -12.07	10.63-12.70
SWW	3	75	34.8-37.5	9.32 -11.50	9.71 -14.24
DUR	3	75	82.1-92.2	11.43-12.46	13.56-14.95

[1] HRS = hard red spring; HRW = hard red winter; SRW = soft red winter; HWW = hard white wheat; SWW = soft white wheat; DUR = durum.

Table 4. Summary of predicting kernel size using near-infrared reflectance as shown by the coefficient of determination (r^2) using three-class partial least squares (PLS) classification model at a wavelength region of 750 to 1900 nm.

Pretreatment	HRS[1]	HRW	SRW	SWW	HWW	DUR
Log(1/R)	0.779[2]a	0.770a	0.771a	0.753a	0.677a	0.729a
MSC on Log(1/R)	0.695b	0.517b	0.728b	0.619c	0.513b	0.627b
1st Derivative	0.711bc	0.388c	0.707b	0.746a	0.457c	0.510c
MSC on 1st derivative	0.671c	0.352d	0.627c	0.525d	0.410d	0.504c
2nd Derivative	0.683c	0.282e	0.575c	0.597c	0.392e	0.389d
MSC on 2nd derivative	0.557d	0.250e	0.411d	0.426d	0.386e	0.319e

[1] HRS = hard red spring; HRW = hard red winter; SRW = soft red winter; HWW = hard white wheat; SWW = soft white wheat; DUR = durum.
[2] Values in the same column which are not followed by the same letter are significantly different ($P < 0.05$).

Table 5. Summary of predicting kernel size using visible reflectance as shown by the coefficient of determination (r^2) using three-class partial least squares (PLS) classification models at a wavelength region of 550 to 750 nm.

Pretreatment	HRS[1]	HRW	SRW	SWW	HWW	DUR
Log(1/R)	0.671[2]a	0.631a	0.534a	0.690a	0.506a	0.560a
MSC on Log(1/R)	0.092d	0.037b	0.144b	0.275b	0.233b	0.064c
1st Derivative	0.406b	0.049b	0.204b	0.276b	0.238b	0.236b
MSC on 1st derivative	0.155c	0.021b	0.078c	0.287b	0.236b	0.144b
2nd Derivative	0.252c	0.055b	0.107b	0.283b	0.247b	0.188b
MSC on 2nd derivative	0.058d	0.008b	0.023c	0.194b	0.105b	0.078c

[1] HRS = hard red spring; HRW = hard red winter; SRW = soft red winter, HWW = hard white wheat; SWW = soft white wheat; DUR = durum.
[2] Values in the same column which are not followed by the same letter are significantly different ($P < 0.05$).

Table 6. Summary of accuracies of three-class partial least squares (PLS) models in the visible and near-infrared region.

Class	No. of kernels[1]			Wavelength region[2]	Correctly classified, %			
	L	M	S		L	M	S	Avg.
HRS[3]	25	25	25	NIR	96.0	72.0	76.0	81.3
				Vis	68.0	68.0	68.0	68.0
HRW	25	25	25	NIR	88.0	84.0	76.0	83.3
				Vis	76.0	56.0	48.0	60.0
SRW	25	25	25	NIR	76.0	84.0	88.0	83.3
				Vis	48.0	84.0	52.0	61.3
SWW	25	25	25	NIR	80.0	80.0	76.0	78.7
				Vis	72.0	80.0	72.0	74.7
HWW	25	25	25	NIR	72.0	80.0	68.0	73.3
				Vis	60.0	84.0	52.0	65.3
DUR	25	25	25	NIR	84.0	84.0	76.0	81.3
				Vis	52.0	72.0	56.0	60.0
Avg.				NIR	82.7	80.7	76.7	80.0
				Vis	62.7	74.0	58.0	64.9

[1] L = large size kernels, M = medium size kernels, S = small size kernels.
[2] NIR = 750-1900 nm, Vis = 550-750 nm.
[3] HRS = hard red spring; HRW = hard red winter; SRW = soft red winter; HWW = hard white wheat; SWW = soft white wheat, DUR = durum.

Table 7. Summary of calibration statistics for partial least squares (PLS) models based on kernel weight at visible and near-infrared region.

Class[1]	n	Region (nm)	r^2	SEC[2]
HRS	75	NIR	0.845	5.34
		Vis.	0.643	8.22
HRW	75	NIR	0.854	2.95
		Vis.	0.571	5.11
SRW	75	NIR	0.802	4.48
		Vis.	0.569	6.64
HWW	75	NIR	0.800	5.79
		Vis.	0.479	9.35
SWW	75	NIR	0.747	6.00
		Vis.	0.651	7.08
DUR	75	NIR	0.799	6.86
		Vis.	0.519	11.04
RED	225	NIR	0.845	4.39
		Vis.	0.513	7.41
WHITE1	150	NIR	0.809	5.48
		Vis.	0.301	10.69
WHITE2	225	NIR	0.763	6.67
		Vis.	0.312	11.60
ALL1	375	NIR	0.832	5.31
		Vis.	0.491	9.47
ALL2	450	NIR	0.810	6.06
		Vis.	0.457	10.73

[1] HRS = hard red spring, HRW = hard red winter, SRW = soft red winter, HWW = hard white wheat, SWW = soft white wheat, DUR = durum, Red = HRS + HRW + SRW, White1 = HWW + SWW, White2 = HWW + SWW + Durum, ALL1 = Red + White1, ALL2 = Red + White2.
[2] SEC = standard error of calibration.

Table 8. Summary of important wavelengths in which kernel weight has a significant effect on reflectance spectra based on multiple linear regression at $P < 0.05$ level.

Class[1]	Wavelength (nm)
HRS	500, 552, 682, 706, 924, 950, 1114, 1148, 1194, 1300, 1376, 1396
HRW	798, 838, 898, 998, 1154, 1160, 1176, 1242, 1292, 1354, 1414
SRW	480, 848, 858, 1112, 1168, 1188, 1268, 1324, 1390, 1058, 1600, 1812
HWW	788, 1084, 1118, 1196, 1528, 1632, 1668
SWW	474, 518,588, 1122, 1172, 1300, 1420, 1674
DUR[2]	450, 482, 658, 712, 740, 762, 826, 1316, 1818
RED	486, 886, 930, 984, 1110, 1148, 1206, 1268, 1330, 1392, 1596, 1858
WHITE1	478, 872, 1006, 1028, 1082, 1116, 1166, 1198, 1370, 1396, 1438, 1450, 1894, 1900
WHITE2	480, 528, 874, 1124, 1172, 1200, 1310, 1370, 1396, 1506, 1634, 1896, 1900
ALL1	464, 882, 1024, 1080, 1110, 1184, 1196, 1398, 1446, 1570, 1628, 1674
ALL2	464, 530, 784, 798, 872, 1020, 1116, 1198, 1308, 1386, 1482, 1630

[1] HRS = hard red spring, HRW = hard red winter, SRW = soft red winter, HWW = hard white wheat, SWW = soft white wheat, DUR = durum, Red = HRS + HRW + SRW, White1 = HWW + SWW, White2 = HWW + SWW + Durum, ALL1 = Red + White1, ALL2 = Red + White2.

[2] The significant level for durum is $P < 0.10$.

Table 9. Summary of kernel weight calibration statistics for six-term multiple linear regression models in the visible and near-infrared region.

Modeled Classes[1]	Wavelength (nm)	n	r^2	SEC[2]
HRS	1104, 1196, 1268, 1300, 1364, 1396	75	0.902	4.54
HRW	998, 1160, 1176, 1240, 1292, 1690	75	0.916	2.37
SRW	926, 992, 1188, 1324, 1600, 1810	75	0.878	3.69
HWW	1010, 1030, 1118, 1164, 1642, 1668	75	0.890	4.49
SWW	518, 712, 880, 1066, 1168, 1420	75	0.874	4.46
DUR	740, 888, 1084, 1126, 1316, 1826	75	0.844	6.52
RED	484, 1108, 1188, 1268, 1334, 1394	225	0.848	4.51
WHITE1	1008, 1028, 1118, 1164, 1438, 1498	150	0.840	5.21
WHITE2	786, 1124, 1164, 1268, 1370, 1634	225	0.762	6.95
ALL1	652, 1028, 1080, 1196, 1398, 1626	375	0.831	5.51
ALL2	876, 1020, 1122, 1198, 1304, 1630	450	0.798	6.58

[1] HRS = hard red spring, HRW = hard red winter, SRW = soft red winter, HWW = hard white wheat, SWW = soft white wheat, DUR = durum, Red = HRS + HRW + SRW, White1 = HWW + SWW, White2 = HWW + SWW + Durum, ALL1 = Red + White1, ALL2 = Red + White2.
[2] SEC = standard error of calibration.

Table 10. The color variations of wheat kernels at different orientation measure as *a** value in the L*a*b* color space.

Wheat Classes	Crease (0°)	90°	Dorsal (180°)
Hard red spring	15.11	18.52	12.29
Hard red winter	19.96	18.09	14.29
Soft red winter	33.00	33.54	26.04
Hard white wheat	15.07	10.41	11.34
Soft white wheat	12.40	10.53	8.16
Durum	13.81	16.32	13.46
Red wheat	22.69	23.37	17.54
White wheat	16.3	12.42	10.99

Table 11. Calibration equation statistics for partial least squares (PLS) models.

Pretreatment	Region (nm)	F[1]	R^2	Correct Classification (%)			
				Red[2]	White	Avg.	SEC[3]
Log(1/R)							
	500-750	4	0.861a[4]	100	99.3	99.7	0.183
	500-1700	7	0.881a	100	100	100	0.169
	750-1900	14	0.768b	96.9	97.3	97.1	0.236
1st derivative							
	500-750	4	0.843a	100	98.7	99.5	0.194
	500-1700	9	0.868a	100	100	100	0.178
	750-1900	12	0.767b	96.9	97.3	97.1	0.237

[1] F = number of partial least squares factors.
[2] Red = hard red spring + hard red winter + soft red winter, White = hard white wheat + soft white wheat. Kernel number of red wheat = 225, kernel number of white wheat =150.
[3] SEC = standard error of calibration.
[4] Values in the same column which are not followed by the same letter are significantly different ($p < 0.05$).

Table 12 . Effect of kernel size on prediction values for red and white kernels where 1=red class and 2=white class (500-1700 nm)

Prediction values	No. of red kernels			No. of white kernels		
	Large	Med.	Small	Large	Med.	Small
<0.55	0	0	5	0	0	0
0.55-0.65	0	2	6	0	0	0
0.65-0.75	0	2	5	0	0	0
0.75-0.85	2	7	10	0	0	0
0.85-0.95	5	12	13	0	0	0
0.95-1.05	7	13	12	0	0	0
1.05-1.15	12	18	13	0	0	0
1.15-1.25	15	9	8	0	0	2
1.25-1.35	14	8	2	0	0	0
1.35-1.45	10	2	1	0	1	1
1.45-1.55	5	2	0	1	1	1
1.55-1.65	2	0	0	1	1	5
1.65-1.75	1	0	0	6	6	13
1.75-1.85	2	0	0	5	7	11
1.85-1.95	0	0	0	12	15	4
1.95-2.05	0	0	0	11	13	2
2.05-2.15	0	0	0	8	5	0
2.15-2.25	0	0	0	6	1	0

Table 13 . Effect of kernel orientation[1] on prediction values for red and white kernels where 1=red class and 2=white class (500-1700).

Prediction values	No. of red kernels			No. of white kernels		
	0°	90°	180°	0°	90°	180°
0.65-0.75	**32**	**19**	**7**	0	0	0
0.75-0.85	**5**	**6**	**3**	0	0	0
0.85-0.95	**4**	**11**	**3**	0	0	0
0.95-1.05	**12**	**15**	**6**	0	0	0
1.05-1.15	**13**	**7**	**5**	0	0	0
1.15-1.25	**3**	**11**	**8**	0	0	0
1.25-1.35	**5**	**5**	**5**	0	0	0
1.35-1.45	**1**	**1**	**9**	0	0	0
1.45-1.55	0	0	**8**	0	0	0
1.55-1.65	0	0	**15**	**2**	0	0
1.65-1.75	0	0	**4**	**4**	**6**	0
1.75-1.85	0	0	**2**	**11**	**6**	**4**
1.85-1.95	0	0	0	**18**	**7**	**13**
1.95-2.05	0	0	0	**15**	**10**	**12**
2.05-2.15	0	0	0	0	**12**	**11**
2.15-2.25	0	0	0	0	**8**	**8**
> 2.25	0	0	0	0	**1**	**2**

[1] 0° = Crease side, 180° = Dorsal side.

Table 14. Summary of the effect of kernel size on single wheat kernel color classification using a calibration equation developed using the crease side.

Range (nm) /Treatment	Red kernels				White kernels				Total Avg.
	L[1]	M	S	Avg.	L	M	S	Avg.	
500-750									
Log 1/R	10.7[2]	0	0	3.6	0	2.0	12.0	4.0	4.0
MSC on Log 1/R	5.3	6.8	1.3	4.9	0	0	6.0	2.0	3.7
1st derivative	5.3	1.3	0	2.2	2.0	0	8.0	3.3	2.4
1st on MSC	5.3	1.3	0	2.2	4.0	0	6.0	3.3	3.7
500-1700									
Log 1/R	10.7	0	0	3.6	0	2.0	12.0	4.0	4.0
MSC on Log 1/R	5.3	0	0	1.8	2.0	0	6.0	2.0	2.1
1st derivative	4.0	0	0	1.3	2.0	0	12.0	4.7	2.7
1st on MSC	6.7	0	0	2.2	4.0	0	6.0	3.3	2.7

[1] For each kernel size, red kernels = 75, white kernels = 50.

[2] Percentage of misclassified kernels (%).

Table 15. Summary of the effect of kernel orientation on single wheat kernel color classification using calibration equation developed using the crease side.

Data Treatment	Crease (0°)			90°			Dorsal (180°)			Total Avg.
/Range (nm)	Red[1]	White[2]	Avg.	Red	White	Avg.	Red	White	Avg.	
500-750										
Log 1/R	1.3[3]	0	0.8	0	0	0	61.3	0	38.6	12.5
MSC on Log 1/R	0	0	0	8.0	0	4.8	10.7	0	6.4	3.7
1st derivative	1.3	0	0.8	4.0	0	2.4	56.0	0	33.6	12.3
1st on MSC	1.3	0	0.8	9.3	0	5.6	10.7	0	6.4	4.3
500-1700										
Log 1/R	0	0	0	0	0	0	32.0	2.0	20.0	6.7
MSC on Log 1/R	0	0	0	0	0	0	2.6	0	1.6	0.5
1st derivative	0	0	0	1.3	0	0.8	45.3	0	27.0	9.3
1st on MSC	2.7	0	1.6	5.3	0	3.2	12.0	0	7.2	4.0

[1,2] For each orientation, red kernels = 75, white kernels = 50.

[3] Percentage of misclassified kernels %.

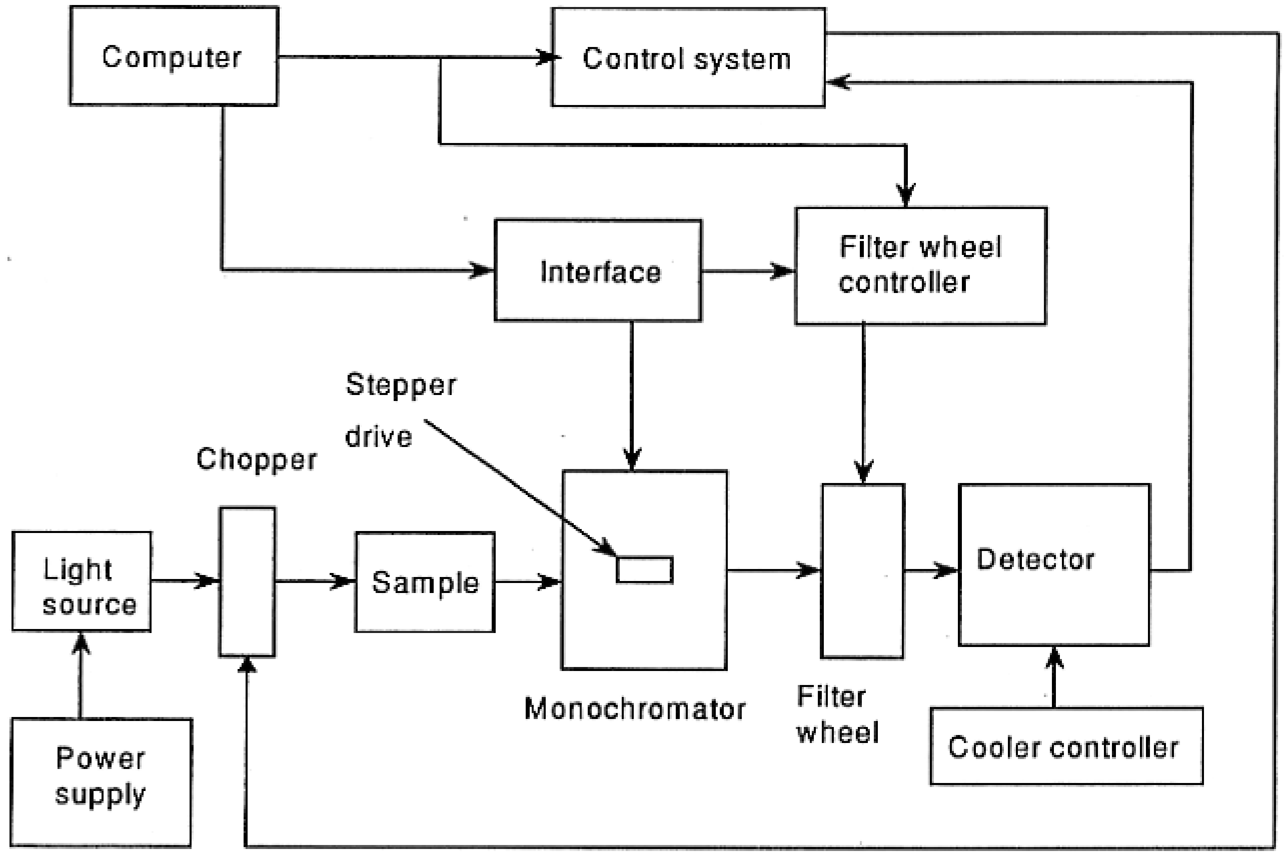

Figure 1. An optical radiation measurement system.

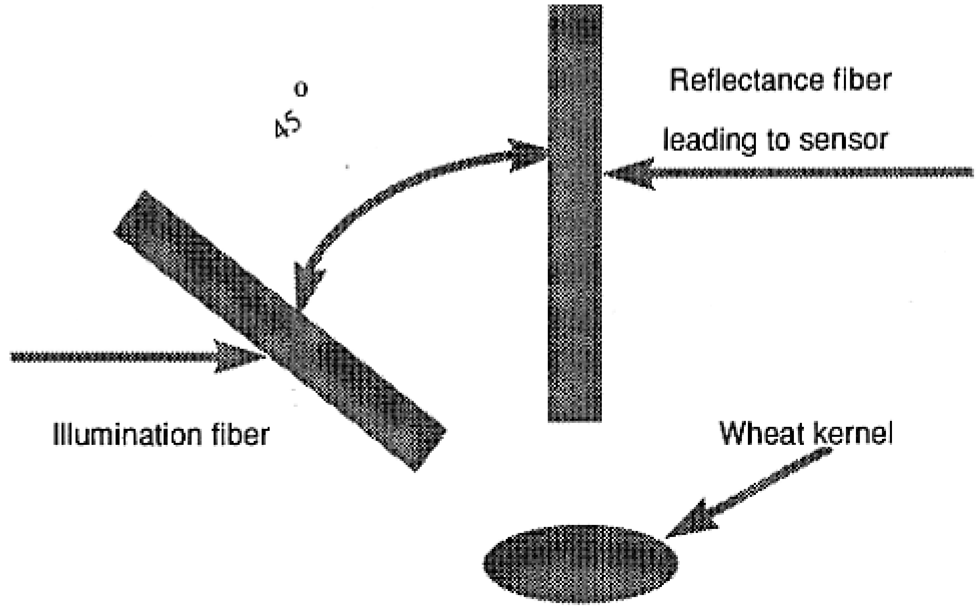

Figure 2. An optical configuration used to quantify the reflectance from single wheat kernels.

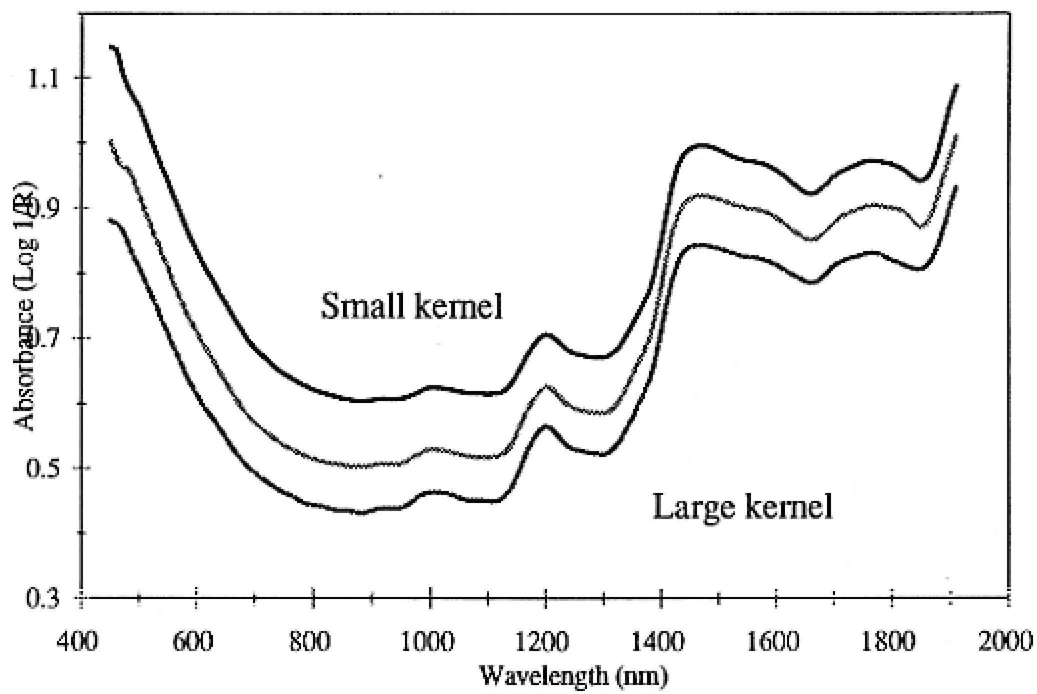

Figure 3. Effect of wheat kernel size on the reflectance spectra in the visible and near-infrared region.

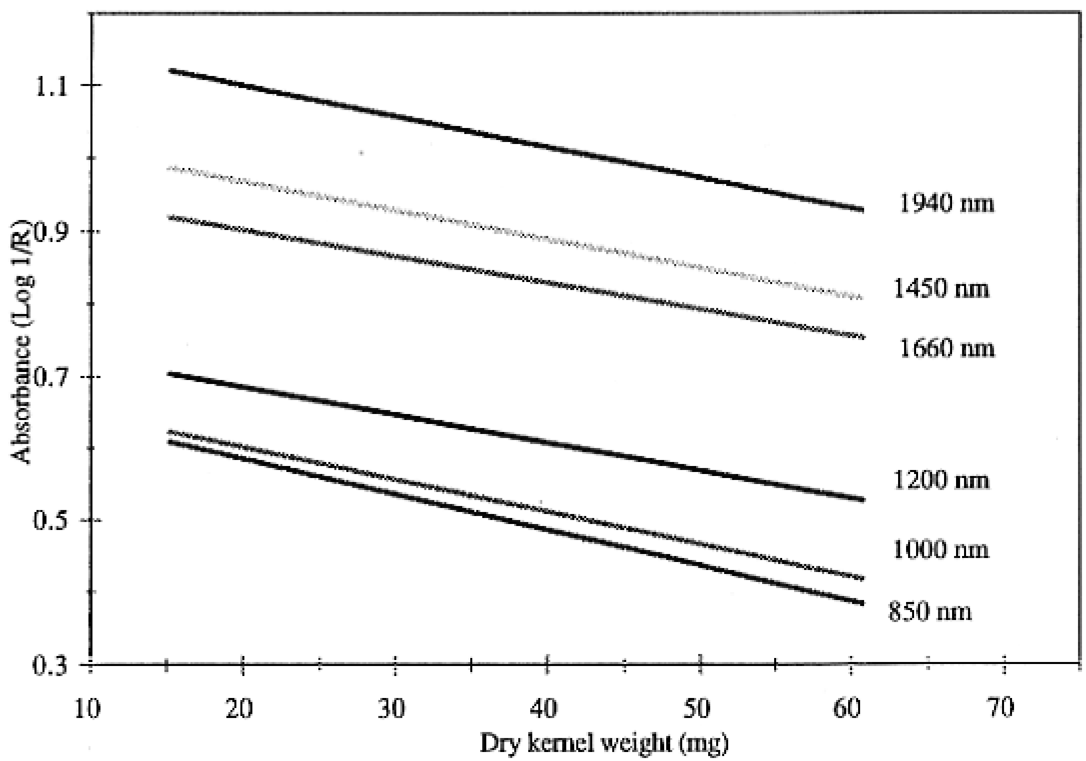

Figure 4. Effect of wheat kernel weight on the reflectance spectra in the near-infrared region.

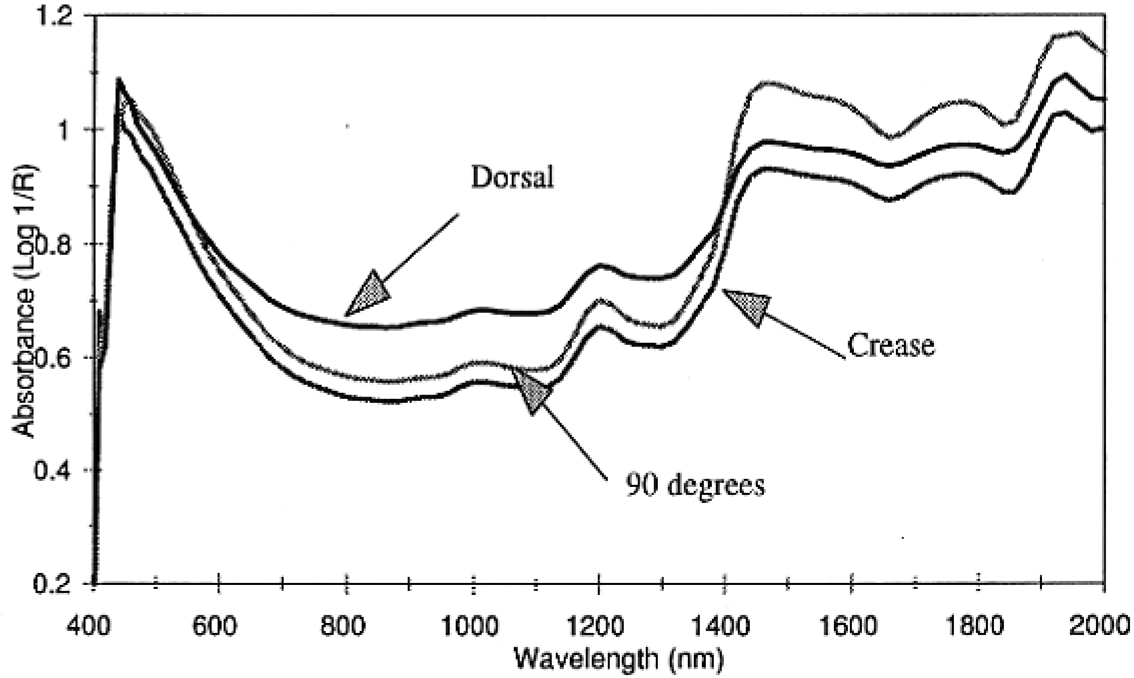

Figure 5. Effect of kernel orientation on the reflectance spectra in the visible and near-infrared region.

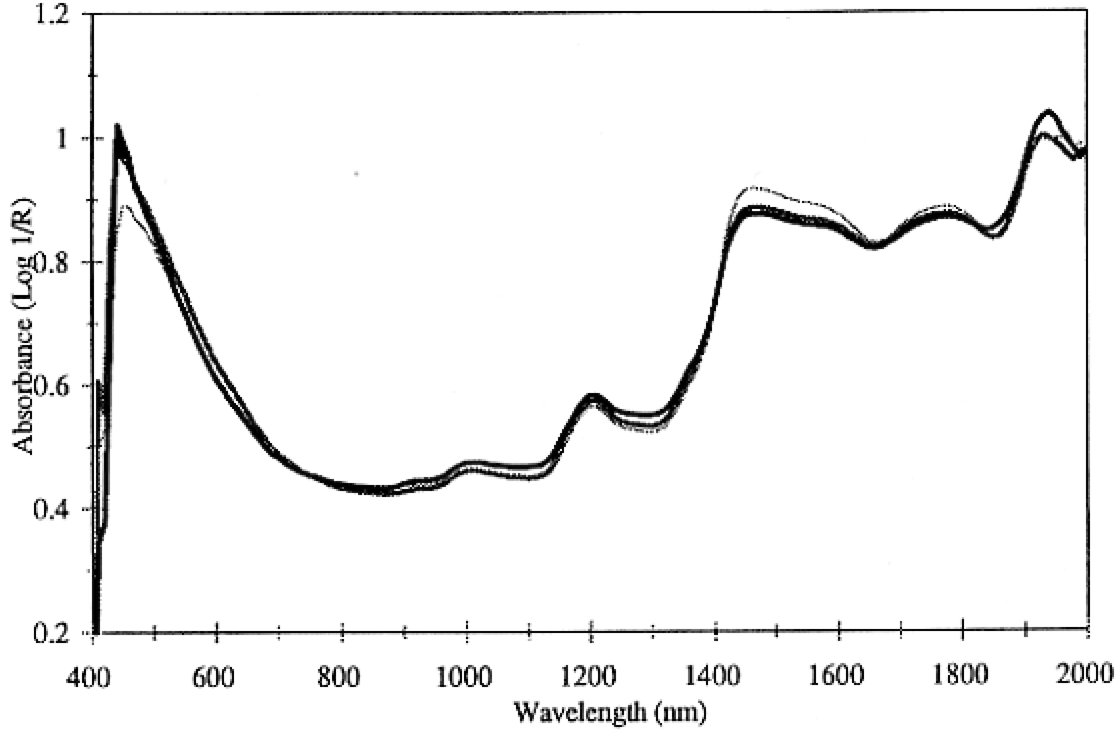

Figure 6. The performance of MSC on reducing the effect of kernel orientation on the reflectance spectra.